Process Parameter Optimization for 3D Printed Investment Casting Wax Pattern and Its Post-processing Technique

Muslim Mukhtarkhanov
Essam Shehab
MD Hazrat ALI (hazratalidu07@yahoo.com)
Kyushu University - Ito Campus: Kyushu Daigaku

Research Article

Keywords: Wax3D, Rheology, Taguchi method, FDM, Casting

Posted Date: May 12th, 2022

DOI: https://doi.org/10.21203/rs.3.rs-1564110/v1

Abstract

This research paper aims to improve the quality of 3D printed parts made of the wax filament by implementing the Taguchi orthogonal array process optimization method. The manufactured parts can be used as cost-effective investment casting patterns. With the Taguchi method, it was concluded that the nozzle temperature has the most effect on the dimensional accuracy of printed parts. In addition, thermal, mechanical, and rheological characterization were performed on the wax filament revealing several important findings. For instance, the rheological studies identified the low viscosity of melted wax at printing temperatures. This resulted in the rough surface of the printed parts. To improve the surface roughness, a post-processing procedure was implemented using a white spirit as a surface smoothing agent.

1. Introduction

Additive Manufacturing (AM) has proved to be a great technology for manufacturing 3D objects that can serve many purposes such as prototypes, fully functional parts, educational tools, or tools that facilitate other types of manufacturing technologies. In particular, the AM was significantly developed to be implemented in the investment casting (IC) industry during the last decades. When AM is used to produce the patterns for metal casting, the manufacturing process is referred to as the rapid investment casting or RIC. Munich et al [1] have mentioned eight types of commercially available AM technologies that are used to produce either wax or non-wax patterns for the IC. Among those methods, the FDM technology is of particular interest for it is a low-cost and widely available product. Additional advantages include the larger build plate and simplicity of the manufacturing process. During the manufacturing process, a wire of plastic/filament is melted and immediately deposited on a flat platform creating a cross-sectional feature of an intended object. The process is continuously repeated, and layers build upon layers creating a solid object. The capabilities of the FDM technology to produce the IC patterns have been studied extensively. Different materials such as general plastics and wax-based filaments are available in the market to be used as patterns for RIC. Among non-wax materials, the ABS showed better performance due to a better surface finish compared to wax filament[2]. The advantage of using non-wax material is in the superior mechanical properties that prevent the pattern from failing during handling or transportation[3][4]. Nevertheless, several downsides have been identified when using non-wax Rapid Prototyping (RP) patterns. They include large thermal expansion during pattern burnout leading to ceramic shell cracking and a higher amount of residual ash [5][6][7][8]. Moreover, the gases generated from burning non-wax patterns, significantly contaminate the mold material, which in turn affects the casting quality. As far as the critical pattern burnout temperature is concerned, when using non-wax patterns, the ceramic shell cracking occurs when the pattern reaches its glass transition temperature (Tg) according to [6]. For ABS the Tg is around 100°C [9] [10] with melting temperature (Tm) ranging from 200 to 240°C. From the physical properties of the ABS filament, it is evident that the burnout procedure is the only proper means for removing the pattern from ceramic mold. In such a case, the material had a negative environmental effect due to wastage and high energy consumption.

As for wax-based filaments, the first materials were developed in the 1990s by Stratasys and had the commercial names ICW04 and MW01. In 1994 Comb et al designed several experiments aiming to modify the composition of wax filaments by mixing wax-based materials ICW04 and MW01 with plastic formulations to improve physical and mechanical properties [11]. In addition, the authors briefly described how the two factorial design was implemented to analyze the effect of printing and envelope temperatures on the surface quality of manufactured parts. Although the study contains meaningful information on the material's properties, the study is void of important details on printability, dimensional accuracy, and surface roughness of parts made of castable wax. The other mention of wax-based FDM material can be found in the review work done by Cheah et al in 2005 [4] where the wax filament was described as the material having inferior mechanical properties. Considering the current market, the list of commercially available "made for casting" filament products with some characteristics is shown in Table 1.

Table 1
Commercially available castable FDM filaments

Commercial Name	Density, g/cm^3	Nozzle Temperature, C	Cost for 1 kg, $
Print2Cast	0.91	140–150	70
MoldLay	N/A	170–180	65
Think3D	N/A	170–180	33
Blue Wax PLA	1.2–1.43	195–240	40
Polycast	1.1	190–230	80
Wax3D	0.98	100–110	34

To the authors' best knowledge, the reports on the effectiveness of the commercial FDM waxes listed in Table 1 are unavailable except for the MoldLay. In 2019 Wang et al performed a topology optimization of a RIC pattern using the MoldLay wax filament [12]. Among a few drawbacks associated with 3D printing wax, a low solidification of material and layer curling were identified as the major downsides. As can be seen from Table 1, most of the castable filaments have printing/melting temperatures much higher than the melting temperature of traditional waxes used in IC. For example, most of the traditional IC waxes have a range of melting temperatures of 60–100°C. Nevertheless, it can be argued that the Wax3D having Tm around 100 ˚C is a potentially better candidate to be used in RIC. Moreover, when working with the material, it has been noticed that it has low viscosity in the molten state which is beneficial for the dewaxing process. As for mechanical properties, the filament has shown high flexibility and softness. Due to low tensile strength and elastic modulus, the manufacturing process is associated with challenges related to finding proper process parameters. Therefore, having considered all the properties of the wax-based FDM filament, the authors have found it necessary to identify the optimal process parameters that can result in successful manufacturing RIC patterns. To achieve the goal, an Orthogonal Array (OA) L9 Taguchi optimization method was implemented with the focus to achieve higher dimensional accuracy.

Higher-dimensional accuracy along with low surface roughness are two main requirements established for the IC patterns. Thus, in addition to dimensional accuracy optimization, the appropriate surface treatment was selected. The research concludes with the work dedicated to finding mechanical, rheological, and thermal properties of the wax filament.

2. Experimental Procedure

2.1. Materials and equipment

Commercially available Wax3D filament from *Filamentarno* was used as a filament wire with ø1.75mm. The melting temperature is 95°C as identified with a dropping point test. The material is of blue color. For 3D printing specimens, a Prusa I3 FDM machine was used.

2.2. Printing process parameter optimization by Taguchi analysis

It has been revealed that many of the properties of Wax3D filament are significantly different from regular plastics used in FDM manufacturing. Therefore, this circumstance necessitates a search for optimal process parameters for manufacturing wax patterns using an FDM machine. In our case, it has been decided to optimize the process parameters for better dimensional accuracy of printed parts. Among existing process optimization tools that were previously successfully applied for the FDM process, Taguchi's parametric design of the experiment proved to be a popular approach according to Omar et al [13]. In Taguchi's method, the so-called Orthogonal Array (OA) fractional factorial design is used to create a design matrix with a selected subset of combinations containing numerous factors at several levels. By performing experiments with suggested combinations, one can identify the significant parameters and choose the optimal combination of parameters' levels that yield the desired outcome. One of the key benefits of using Taguchi's method is that it allows minimizing the number of experiments significantly. Based on Taguchi's design, nine experiments were needed to investigate the influence of three parameters with three control levels. As for the parameters, the layer thickness, nozzle temperature, and extrusion velocity were chosen as shown in Table 2. From Table 2 it can be noticed that the tested temperatures are between 105 and 115°C. This is because printing at lower temperatures increases the possibility of emerging defects such as delamination and bad bed adhesion. On the other hand, printing above 115°C caused the nozzle to clog due to heat creep.

Table 2
Selected parameters and levels for Taguchi analysis

Input Parameters	Symbol	Level 1	Level 2	Level 3
Nozzle temperature, ˚C	I	105	110	115
Layer thickness, mm	II	0.2	0.25	0.3
Extrusion velocity, mm/sec	III	40	50	60

A Minitab software was used to perform calculations of Taguchi analysis. It should be noted that the FDM process has a considerable number of controllable parameters to choose from and, therefore, it is difficult to select the most important factors for designing the experiment. To identify the list of parameters the preliminary work was done through 3D printing numerous simple geometry samples and studying the literature on the subject. The geometry chosen for the analysis is a cube with dimensions of 20×20×20 mm (L×W×H). Other important printing parameters which were kept constant are:

- bed temperature, 65 ˚C;
- wall count, 2;
- top/bottom walls, 4;
- the nozzle diameter, 0.4 mm;
- infill pattern, concentric with 80% fill.

The dimensions were measured using a digital caliper with an error of ± 20μm. The measured sides are height H (z print direction) and width W (x print direction). In total, twenty-seven parts were manufactured and for each experiment, the average of deviations of three samples was recorded. The values for the average, standard deviations, and ranges are shown in Table 3.

Table 3
The results of measurements taken from 3d printed 20×20×20mm parts

Experiment #	Average value of error, mm		Range, mm		Standard deviation, mm	
	Height	Width	Height	Width	Height	Width
1	0.14	0.07	0.19	0.09	0.10	0.05
2	0.34	0.17	0.27	0.3	0.15	0.15
3	0.21	0.18	0.1	0.05	0.06	0.03
4	0.18	0.03	0.07	0.04	0.04	0.02
5	0.26	0.02	0.09	0.02	0.05	0.01
6	0.28	0.02	0.08	0.03	0.04	0.02
7	0.11	0.12	0.22	0.18	0.12	0.10
8	0.27	0.23	0.23	0.07	0.12	0.04
9	0.16	0.07	0.16	0.03	0.08	0.02

As far as a Signal-To-Noise (S/N) ratio is concerned, “the lower the better” response was chosen because the preference is to have a low dimensional deviation. By finding the S/N ratio it is possible to identify the effect of input parameters on the responses. An Eq. (1) was used to find the S/N ratio as follows:

$$\frac{S}{N} = -10\log_{10}\left[\frac{1}{n}\sum_{i=1}^{n} y_1^2\right]$$

1

here, n is the number of repetitions and y is the characteristic under consideration. The calculated S/N ratio values are shown in Table 4.

Table 4
Calculated S/N ratio values

No	I	II	III	S/N ratio for height	S/N ratio for width
1	105	0.2	40	17.07	22.69
2	105	0.25	50	11.05	15.22
3	105	0.3	60	16.28	15.05
4	110	0.2	50	14.73	31,48
5	110	0.25	60	13.7	35,56
6	110	0.3	40	13.15	32.64
7	115	0.2	60	19.17	18.41
8	115	0.25	40	13.28	12.64
9	115	0.3	50	20	9.80

To identify the degree of importance of each parameter for three corresponding outputs, the analysis of variance (ANOVA) statistical tool was implemented. The significance of factors can be supported by calculated p values. A threshold value for p was chosen as 0.05 indicating that any factor's p-value higher than this number can render it as insignificant.

2.3. Characterization

2.3.1 Thermal

The thermogravimetric (TGA) and differential scanning calorimetry (DSC) analyses were performed using simultaneous DSC-TG analyzer STA 6000 from Perkin Elmer. The sample was heated from 25 ˚C to 600 ˚C at a rate of 10 ˚C/min. As a flowing agent, Nitrogen at a 20 ml/min flow rate was applied. The curves such as heat flow/temperature and weight loss/temperature were obtained.

2.3.2 Mechanical

To estimate the mechanical properties of the Wax3D printed part, five tensile samples were manufactured and tested according to ASTM D638. The values of Ultimate Tensile Strength (UTS) and Young's Modulus

were calculated. The specimens were 3D printed with 100% infill using a concentric infill pattern with layers aligned parallel to the load axes. A Tinius Olsen H25KS tensile machine was used with a constant rate of 5 mm/min.

2.3.3 Rheological

A modular compact rotational rheometer MCR 102 from Anton Paar was used to perform rheological characterization with a set of 50 mm cone-plate measuring systems. To identify the limits of the linear viscoelastic region, strain sweeps up to 10% were performed. After that, a frequency sweep test took place with an angular frequency range from 100 to 0.1 rad/sec at a constant amplitude of 5%. The 5% value is within the viscoelastic region as was identified during the small amplitude oscillatory shear (SAOS) test. The found values are storage and loss moduli as well as the complex viscosity. A time-temperature superposition method was also used to find values at higher and lower shear rates taking 110 ˚C as a reference temperature.

3 Results And Discussion

3.1 Taguchi analysis results

Taguchi OA process optimization analysis has revealed several important findings. The main effect plots for the S/N ratio are shown in Figs. 1 and 2. It is clear from the main effect plots that the dimensional accuracy in the horizontal direction is mostly influenced by the nozzle temperature, whereas the accuracy in the vertical direction depends on the layer thickness. The ANOVA analysis results in Tables 5 and 6 show that with a high confidence level of p = 0.022 the dimensional accuracy in the horizontal direction is influenced by printing temperature and 110 ˚C is the optimal value. As for the influence level of the rest of the factors, the high values of the p number suggest their small effect on the output. It is worthy to highlight that supported by Taguchi analysis, thermal and rheological characterization have helped to find the optimal temperature which is equal to 110 ˚C.

Table 5. ANOVA results for part's height accuracy

Source	Degree of freedom	Sum of squares	Mean square	F	P	Contribution, %	R-sq, %
Nozzle temperature	2	21,210	10,605	1,96	0,338	30	84.72
Layer thickness	2	33,345	16,672	3,08	0,245	47.1	
Extrusion velosity	2	5,368	2,684	0,50	0,668	7.6	
Residual Error	2	10,810	5,405			15.3	
Total	8	70,734				100	

Table 6. ANOVA results for part's width accuracy

Source	Degree of freedom	Sum of squares	Mean square	F	P	Contribution, %	R-sq, %
Nozzle temperature	2	643,15	321,576	43,66	0,022	88.3	97.98
Layer thickness	2	38,52	19,259	2,61	0,277	5.3	
Extrusion velosity	2	32,16	16,082	2,18	0,314	4.4	
Residual Error	2	14,73	7,365			2	
Total	8	728,57				100	

3.2 Thermal analysis of Wax3D

The DSC is one of the most effective analytical tools for wax and other polymer materials which helps to identify thermal properties such as melting point and glass transition temperature. A DSC curve shown in Fig. 3 for the Wax3D filament indicates a presence of a melting range starting at 46 and ending at 130 ˚C. This is most probably due to the fact that the Wax3D represents a blend of different waxes. Nevertheless, a distinguishable peak can be observed at 110 ˚C. It is interesting to note that the Taguchi optimization method results have shown the printing temperature of 110 ˚C to be an optimal value for better dimensional accuracy. In addition, it is evident that such broad melting point ranges are similar to those found in polyethylene-based waxes [14]. Thus, a high probability exists that the Wax3D has polyethylene in its content. Polyethylene waxes can have higher hardness and melting point depending on the crystallinity level according to Glenda Webber[14].

The TGA weight loss curve is presented in Fig. 4. The temperature of 0.5% material decomposition at 327.2 ˚C for Wax3D is shown in Table 7. A non-apparent two-stage degradation pattern is observed, and the degradation start of low molecular weight components can be identified during the first step of degradation. From the analysis results, the wax filament may be Polyethylene based synthetic composite wax due to similarities found in the works of Gill et al [15] and Glenda Webber [14]. For example, Glenda Webber has performed the DSC analyses on several commercial HDPE waxes and found melting temperature ranges that are very close to what was found in the current research.

Table 7
Values obtained from TGA

Material	On-set T, ˚C	T at 5% loss, ˚C	Weight loss for the first decomposition, %	T at 50% weight loss, ˚C
Wax3D	318.9	327.2	24.51	440.2

3.3. Mechanical properties of Wax3D

The results of the tensile strength test are shown in Table 8. It has been indicated that the Wax3D has tensile strength and Young's modulus considerably lower compared to general 3D printing plastics such as PLA and ABS. For example, Adrian et al [16] reported the UTS for PLA and ABS plastics to be close to 55 and 42 MPa respectively. As for Young's moduli, the values were found to be 1.94 (PLA) and 1.49 GPa (ABS). By comparing the data, we can see that the commonly used FDM plastics exceed the values of the wax filament by around 20 times in tensile strength and 10 times in modulus of elasticity. This means that both advantages and drawbacks can be found when working with the Wax3D filament. For instance, low elasticity is advantageous for avoiding ceramic shell cracking. On the other hand, the challenge exists when manufacturing parts with thin sections. Nonetheless, it should be noted that the strength of popular IC wax such as B140 is inferior to Wax3D having the UTS value equal to 0.98 MPa[17]. The tested Wax3D specimens representing almost brittle failure mode are shown in Fig. 5 and the average nominal strain at break was found to be 11.42%.

Table 8
The UTS and Young's modulus for Wax3D samples

Material	UTS (MPA)	Young's modulus (MPa)
Wax3D	2.84	151.5

3.4. Rheological characteristics of Wax3D

According to Gilmer et al [18], the polymer melts may undergo a shear rate that may exceed 500 s-1 during the extrusion stage. Thus, the molten wax was exposed to shear rates between 100 and 0.1 s-1 and time-temperature superposition was applied to extend the shear rate boundaries from 0.01 to 1000 s-1. The reference temperature was chosen to be 110 ˚C because it is the optimal printing temperature according to Taguchi's analysis.

As was pointed out by Arit et al [19], the SAOS test is extensively used in analyzing the rheological properties of extrudates at shear rates close to zero. At a stage when an extrudate was just deposited on the print bed, it experiences a low shear rate which may cause some amount of deformation. Thus, the extrudate must have a sufficient level of viscosity to withstand large form distortions. The frequency sweep test results for Wax3D are shown in Fig. 6.

From Fig. 6 (a) it is evident that the material behaves more like viscous liquid at low shear rates since the viscous modulus is higher than the elastic modulus G"">G'. According to Fig. 6 (b), the complex viscosity (□*) values of the Wax3D are within 44 and 163 Pa*s. In contrast, Gianluca et al [20] have found that within the same range of angular frequency, the □* values for PLA are in the range of 1000 and 3000 Pa*s. Likewise, the elastic and storage moduli of PLA can be one order of magnitude larger than the Wax3D[20]. The test results also showed that between 130 and 150°C, the viscosity values are quite low and, therefore, the pattern made from this material can be dewaxed using autoclave boilers that are used extensively in the traditional IC industry. Thus, the 3D printed wax patterns can be introduced to the traditional IC process without modifying the technological sequence. However, the low viscosity and

moduli values are probably the primary reasons for the printed parts to have high surface roughness values.

4. Post-processing For Surface Roughness Improvement

It is a well-known fact that IC manufacturing produces a high-quality surface finish due to the application of ceramic slurry coating. Therefore, it is required for the pattern as well to have superior surface quality. In the case of 3D printed parts, surface roughness was always an issue due to stair-stepping effect. The problem is aggravated even more for materials having low viscosity values at the molten state such as wax. For example, Fig. 7 shows a 20×20×20 mm wax cube with the presence of rippling on the side surface. The measured Ra values using the portable surface roughness tester showed the values in the range of 25–39 μm. The parts tested are the cubes used in the Taguchi analysis.

To overcome the issue of low surface quality, it was decided to apply chemical treatment using a proper agent that can partially dissolve the material. From the literature, numerous works can be found on enhancing popular plastics such as PLA and ABS through chemical treatment. For example, one popular method for improving the surface roughness of ABS parts is the use of an acetone bath. Jayanth et al [21] have found that immersing the printed ABS parts in acetone for several minutes significantly decreases the Ra value from 9.42 to 0.84 μm. However, it was noticed that a longer immersion time may impair mechanical properties. In the current case, the same approach can be utilized by choosing different chemicals such as a white spirit. White spirit is known as the wax dissolver, therefore, it can be used to remove the surface irregularities provided sufficient immersion time is applied. To see the effect of the chemical on the surface, the wax cubes were immersed in a white spirit bath for several periods of time. All the cubes were manufactured using the same process parameters to ensure equal starting conditions are maintained for all samples. However, the Ra values of untreated samples were not equal and varied between 25.1 and 28.3 μm. Nevertheless, the experiment was conducted using three immersion time periods such as 1, 3, and 5 min. The experiments showed that holding for more than 10 min has a negative effect on the object and delamination might occur. On the other hand, a significant improvement was noticed when using 5 min immersion time with the subsequent wiping of the surface using a soft tissue. Figure 8 shows the optical microscopic images of chemically treated and untreated parts. It should be noted that regardless of the magnitude of starting Ra value, the Ra value after 5 min immersion was approximately 3.2 μm ± 0.05 μm for all samples.

5. Conclusion

By implementing Taguchi process optimization, it was possible to identify that printing temperature followed by layer thickness are the most influential process parameters to ensure higher dimensional accuracy of wax patterns manufactured through FDM AM technology. Interestingly, the apparent melting peak at 110 ˚C identified by DSC analysis, coincides with the optimal printing temperature found by Taguchi analysis. Thermal analysis by means of DSC revealed a broad range of melting points which can identify the wax-based filament as a blend of waxes with a high probability of the polyethylene being

present in its content. In addition, no glass transition temperature was identified during the analysis with a noticeable melting peak at approximately 110 ˚C. The absence of Tg is advantageous since it eliminates the sharp transition from a solid to a soft state. Mechanical analysis on 3D printed samples shows that UTS and Young's modulus are significantly lower compared to ABS and PLA plastics. However, the mechanical properties of Wax3D are superior in comparison to some commercially available IC waxes. Nevertheless, to manufacture thin wall objects the stiffness of the Wax3D material should be improved. As for rheological characterization employing a rotational rheometer, the results show that the Wax3D melt has low complex viscosity and viscoelastic moduli at printing temperature compared to popular FDM polymer melts. On the one hand, the low viscosity of the material is beneficial when it comes to dewaxing the pattern during the RIC process. On the other hand, it greatly increases surface roughness. Nevertheless, it was found that by applying the chemical treatment on the surface of the printed part, the surface quality can be improved to reach the value of Ra = 3.2 μm. As for the chemical agent, the white spirit has proved to be effective material. Future work might include an investigation aiming to address the quality of castings made with the help of 3D printed wax patterns and the selection of proper dewaxing procedures.

This study is a part of an ongoing research project which will also evaluate the quality of castings produced using Wax3D patterns.

Declarations

a. Funding

The research grant is provided by Nazarbayev University, Kazakhstan.

b. Conflicts of interest/Competing interests (include appropriate disclosures)

Not applicable

c. Availability of data and material (data transparency)

Data and material can be provided upon request.

d. Code availability (software application or custom code)

Not applicable

e. Ethics approval (include appropriate approvals or waivers)

Not applicable

f. Consent to participate (include appropriate statements)

Not applicable

g. Consent for publication (include appropriate statements)

Not applicable

h. Authors' contributions

M. Mukarkhanov has generated the idea, created a methodology, and written the original draft. **E.Shehab** has supervised the research. **M.H.Ali** has generated the idea, revised the draft, and finalized the article.

References

1. Chhabra M, Singh R (2011) Rapid casting solutions: A review. Rapid Prototyp J 17(5):328–350. doi: 10.1108/13552541111156469
2. Harun WSW, Safian S, Idris MH (2009) Evaluation of ABS patterns produced from FDM for investment casting process. WIT Trans Eng Sci 64:319–328. doi: 10.2495/MC090301
3. Blake P, Fodran E, Koch M, Menon U, Priedeman B, Sharp S (1997)“FDM of ABS patterns for investment casting,”
4. Cheah CM, Chua CK, Lee CW, Feng C, Totong K (2005) Rapid prototyping and tooling techniques: A review of applications for rapid investment casting. Int J Adv Manuf Technol 25:3–4. doi: 10.1007/s00170-003-1840-6
5. Kumar P, Ahuja IPS, Singh R (2012) Application of fusion deposition modelling for rapid investment casting - A review. Int J Mater Eng Innov 3:3–4. doi: 10.1504/IJMATEI.2012.049254
6. Wang S, Miranda AG, Shih C (2010) A study of investment casting with plastic patterns. Mater Manuf Process 25(12):1482–1488. doi: 10.1080/10426914.2010.529585
7. Singh S, Kumar P, Singh J (2021) “An approach to eliminate shell cracking problem in fused deposition modeling pattern based investment casting process,” in *IOP Conference Series: Materials Science and Engineering*, vol. 1091, no. 1, p. 12035
8. Mukhtarkhanov M, Perveen A, Talamona D (2020) Application of Stereolithography Based 3D Printing Technology in Investment Casting. Micromachines 11(10):946
9. Yin J, Lu C, Fu J, Huang Y, Zheng Y (2018) Interfacial bonding during multi-material fused deposition modeling (FDM) process due to inter-molecular diffusion. Mater Des 150:104–112. doi: 10.1016/j.matdes.2018.04.029
10. Baca D, Ahmad R (2020) The impact on the mechanical properties of multi-material polymers fabricated with a single mixing nozzle and multi-nozzle systems via fused deposition modeling. Int J Adv Manuf Technol 106:9–10. doi: 10.1007/s00170-020-04937-3
11. Comb J, Priedeman W, Turley PW (1994)“FDM® Technology process improvements,”
12. Wang J, Sama SR, Lynch PC, Manogharan G (2019) “Design and topology optimization of 3D-printed wax patterns for rapid investment casting,” *Procedia Manuf.*, vol. 34, no. January, pp. 683–694, doi: 10.1016/j.promfg.2019.06.224

13. Mohamed OA, Masood SH, Bhowmik JL (2015) Optimization of fused deposition modeling process parameters: a review of current research and future prospects. Adv Manuf 3(1):42–53. doi: 10.1007/s40436-014-0097-7
14. Webber GV (2000) “Wax characterisation by instrumental analysis,”Stellenbosch University,
15. Gill YQ, Saeed F, Shoukat MH, Irfan MS, Abid U (2021) A Study on the Dewaxing Behavior of Carbon-Black-Modified LDPE–Paraffin Wax Composites for Investment Casting Applications. Arab J Sci Eng 46(7):6715–6725
16. Rodríguez-Panes A, Claver J, Camacho AM (2018) The influence of manufacturing parameters on the mechanical behaviour of PLA and ABS pieces manufactured by FDM: A comparative analysis. Mater (Basel) 11(8):1333
17. Pattnaik S, Karunakar DB, Jha PK (2012) Developments in investment casting process—a review. J Mater Process Technol 212(11):2332–2348
18. Gilmer EL, Mansfield C, Gardner JM, Siochi EJ, Baird DG, Bortner MJ (2019) Characterization and analysis of Polyetherimide: realizing practical challenges of modeling the extrusion-based additive manufacturing process. ” in Polymer-Based Additive Manufacturing: Recent Developments. ACS Publications, pp 69–84
19. Das A, Gilmer EL, Biria S, Bortner MJ (2021) Importance of Polymer Rheology on Material Extrusion Additive Manufacturing: Correlating Process Physics to Print Properties. ACS Appl Polym Mater 3(3):1218–1249. doi: 10.1021/acsapm.0c01228
20. Cicala G, Giordano D, Tosto C, Filippone G, Recca A, Blanco I (2018) Polylactide (PLA) filaments a biobased solution for additive manufacturing: Correlating rheology and thermomechanical properties with printing quality. Mater (Basel) 11(7):1191
21. Jayanth N, Senthil P, Prakash C (2018) Effect of chemical treatment on tensile strength and surface roughness of 3D-printed ABS using the FDM process. Virtual Phys Prototyp 13(3):155–163

Figures

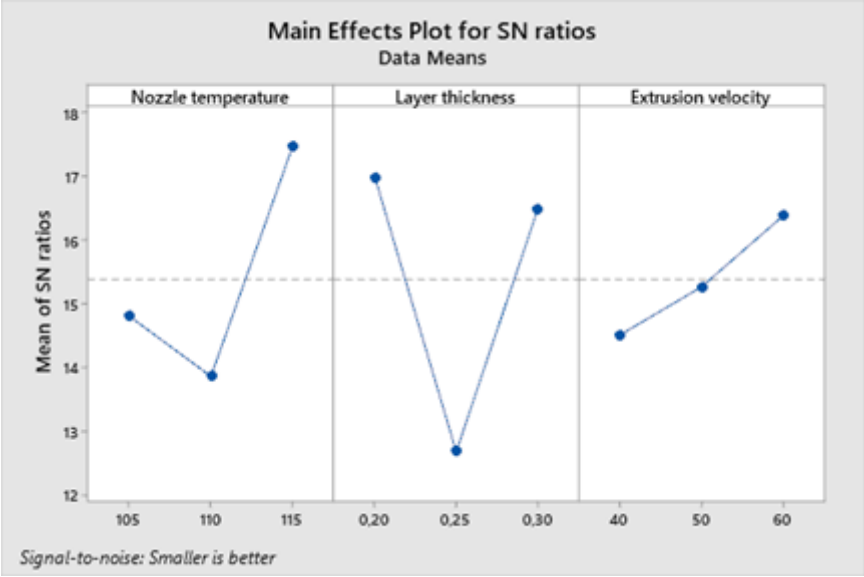

Figure 1

Main effects plot for S/N regarding part's height accuracy

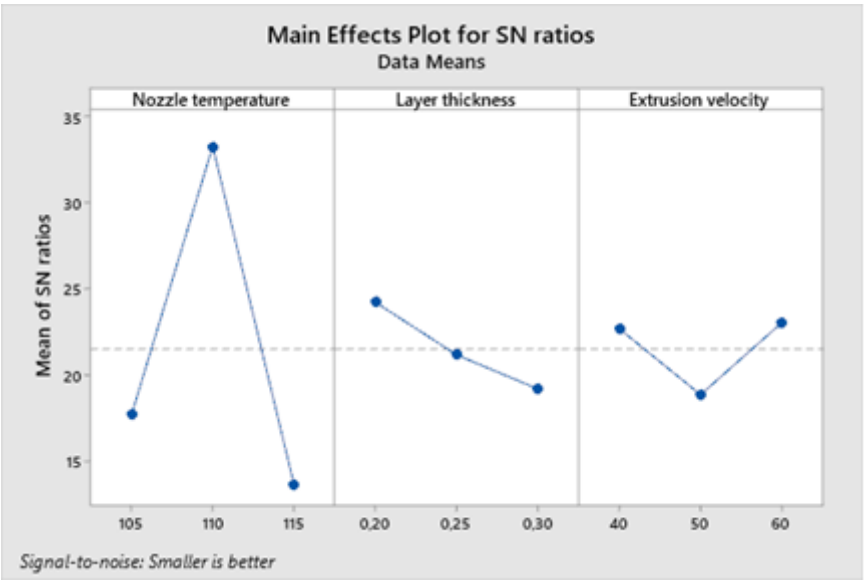

Figure 2

Main effects plot for S/N regarding part's width accuracy

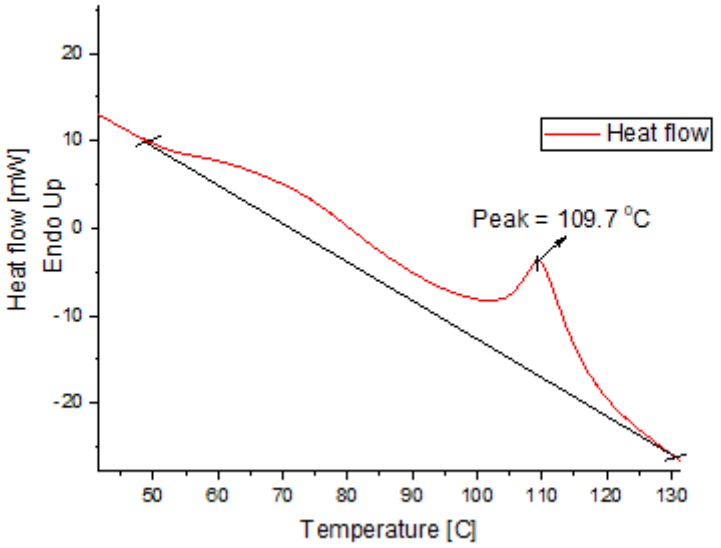

Figure 3

DSC curve for Wax3d filament

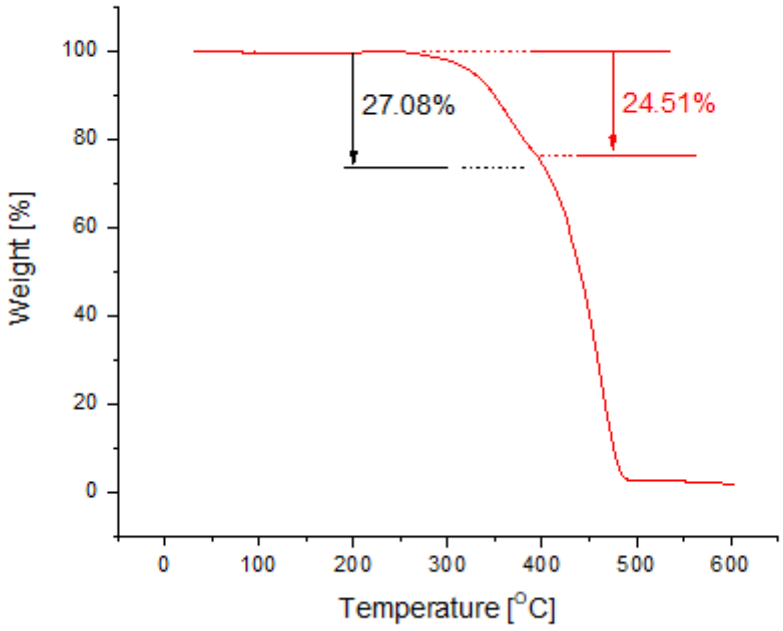

Figure 4

Thermogravimetric analysis curves of Wax3D filament

Figure 5

Fractured tensile samples of Wax3D

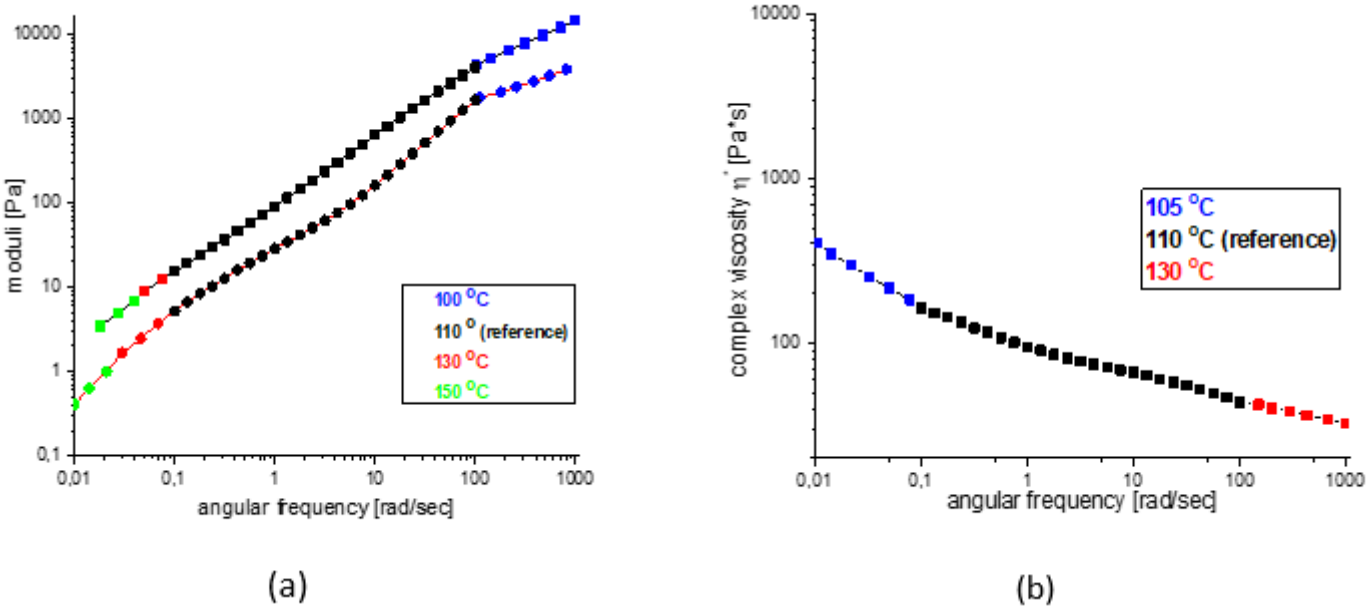

Figure 6

(a) Loss (rectangles) and storage (circles) moduli. (b) complex viscosity values. Time-temperature superposition was applied to a temperature range from 100 to 150 ˚C

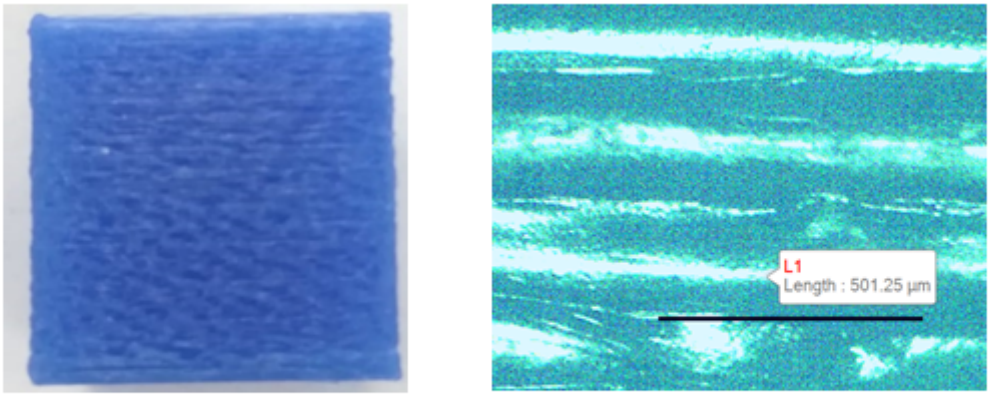

(a) (b)

Figure 7

(a) 3D printed wax cube with visible ripples on the side surface; **(b)** magnified view of the surface

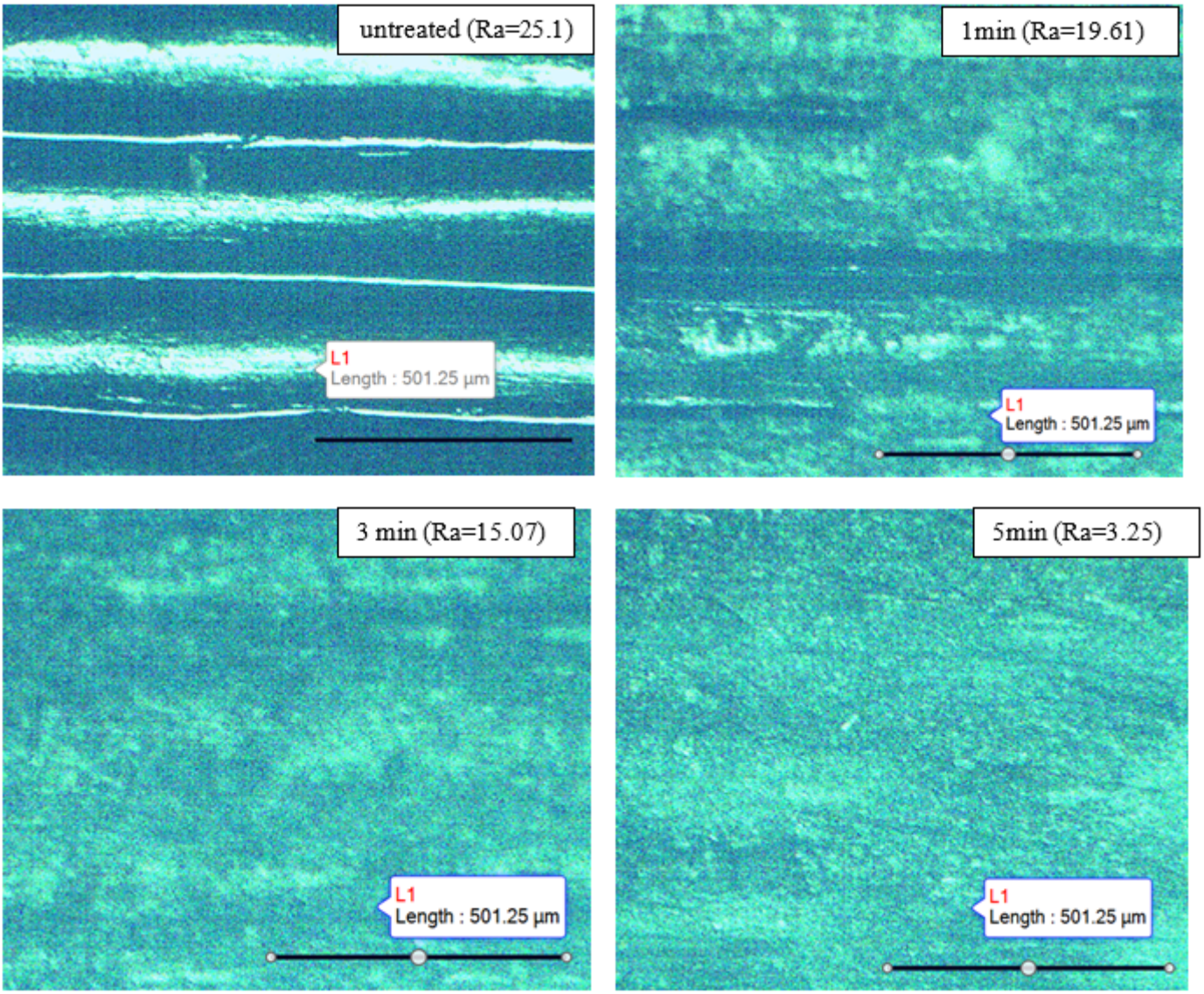

Figure 8

Optical microscopic images of treated and untreated wax parts. The immersion time is indicated at the upper right corner of each image